Nevada Bureau of Mines and Geology Open-File Report 18-2

Subsurface Trenching Investigation in Support of the Barrick Goldstrike N. Carlin Trend Structure Project

by

Richard D. Koehler and Colin M. Chupik

Nevada Bureau of Mines and Geology, University of Nevada, Reno

2018

INTRODUCTION

This report presents the findings of a surface geomorphic assessment and subsurface geologic trenching investigation conducted by the Nevada Bureau of Mines and Geology through a scientific research agreement with the Open Pit Mine Exploration (Mine X) group of Barrick Goldstrike Mine. The project site is located in the Tuscarora Mountains in Elko County, Nevada within the northern Carlin trend. Specifically, the site is within the Santa Renia Fields 7.5' topographic quadrangle about 45 mi (72 km) north of Carlin, Nevada and 10 mi (16 km) southwest of Tuscarora, Nevada (figure 1). The site is characterized by gentle slopes and rolling topography with bedrock cored hills and narrow alluvial valleys (figures 2A and 2B). Access to the project area is by a county road (Dunphy Road), which extends from U.S. Interstate 80 near exit 254 north through Boulder Valley between the Sheep Creek Range and Richmond Mountain to the site.

The purpose of the investigation was to evaluate the presence or absence of Quaternary active faults in the project area and to document the local bedrock structure and stratigraphy and Quaternary cover sediments exposed in the trenches. The results are intended to help refine previous bedrock mapping at the site and provide information that may contribute to improvement of regional and local structural models. Description and measurement of discontinuities, shears, and bedrock lithologies exposed in the trenches and analyses of rock chips (being conducted by Barrick geologists concurrently with this project) will contribute to future Barrick assessments of mineralization at depth and delineation of potential future drill targets.

The scope of the investigation included a review of previous geologic mapping, review of previous data related to active tectonic faults in the project area, inspection of imagery to evaluate site geomorphology and youthful tectonic deformation, excavation and documentation of two approximately 1500-ft (457-m)-long trench exposures, and dissemination of project results to Barrick Goldstrike Mine in this report. As part of the scientific agreement, a graduate student was trained in subsurface documentation techniques.

CARLIN TREND BACKGROUND

The Carlin trend is a 60-km-long zone of gold producing areas in north-central Nevada and represents the largest and most productive accumulation of gold deposits in North America (Teal and Jackson, 1997). The geology and mineral potential of the Carlin trend has been extensively studied over the last 50 years and various interpretations on the history and origin of the mineralization have been previously described and are beyond the scope of this report. Ressel and Henry (2006) provide a summary of these investigations and a comprehensive compilation of relevant references. Host rocks in the Carlin trend are Paleozoic sedimentary rocks, predominantly Devonian and Silurian carbonate rocks. Gold mineralization also occurs in Silurian and Ordovician chert and argillite, and Jurassic and Eocene intrusive rocks. In general, igneous episodes in the Jurassic, Cretaceous, Eocene, and Miocene may have all affected the development of gold mineralization with the greatest mineralization in the Eocene (Ressel and Henry, 2006). Scientific research has not reached consensus on the sources of heat and fluids that contribute to the concentration of gold deposits in the trend. Structural influences on gold mineralization throughout the Carlin trend include high-angle, northwest-striking fault sets that serve as primary fluid conduits and are commonly filled by lamprophyric and monzonitic dikes and high-angle, northeast-striking faults that serve as secondary conduits, particularly along fault intersections (Teal and Jackson, 2002).

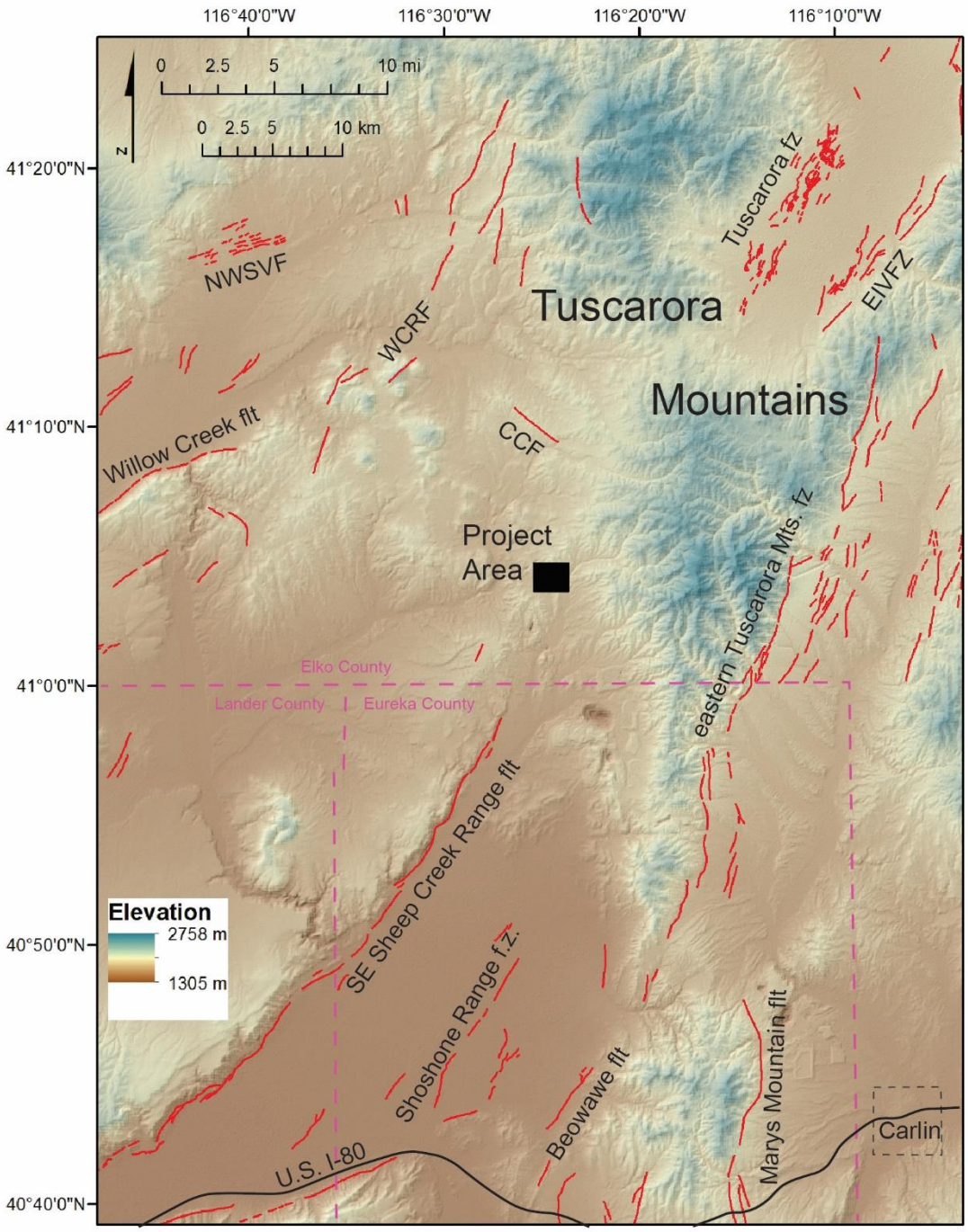

Figure 1. Digital elevation model of the Tuscarora Mountains and project region. Project area shown by black square. NWSVF, unnamed faults northwestern Squaw Valley; WCRF, unnamed fault zone near Willow Creek Reservoir, CCF, unnamed fault near China Camp; EIVFZ, eastern Independence Valley fault zone.

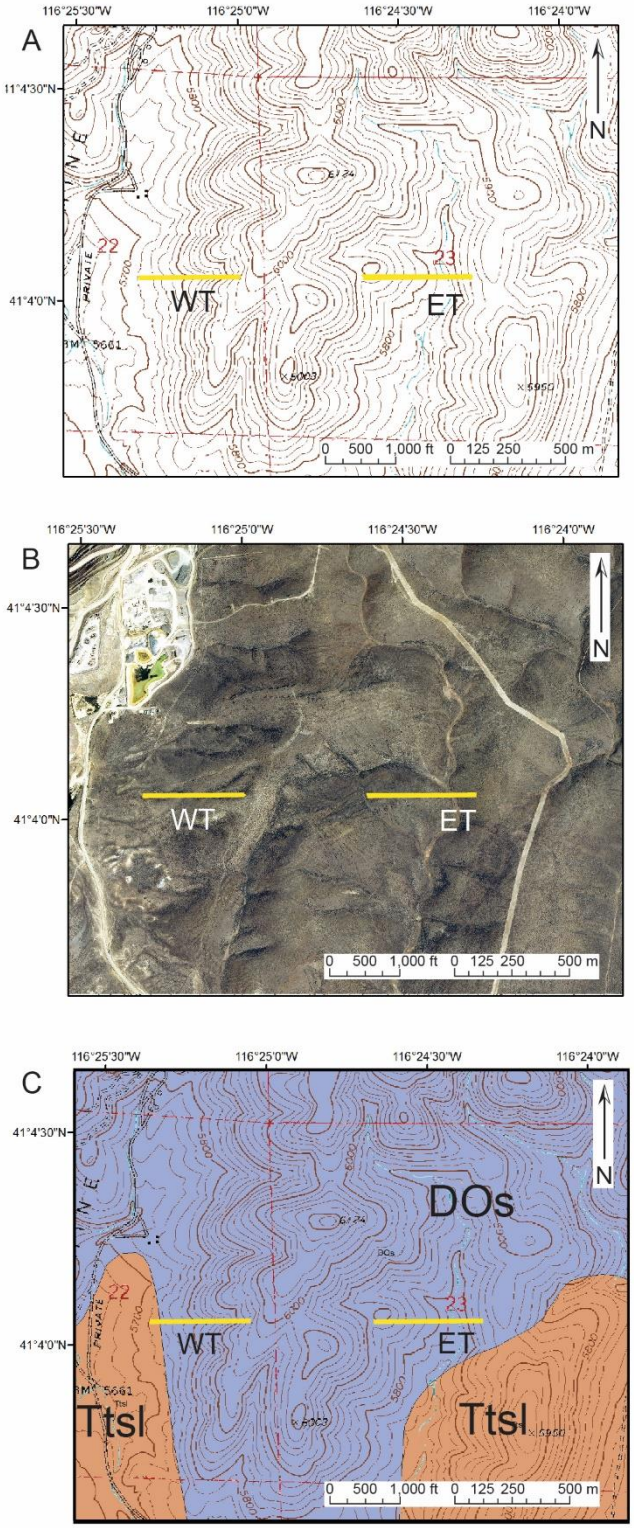

Figure 2. Project area. (A) Santa Renia Fields quadrangle topographic map, (B) 2013 NAIP imagery from the W.M. Keck Earth Sciences and Mining Research website, and (C) geologic map taken from Coats (1987). Trench locations shown by yellow lines. DOs, Devonian mudstone, shale, chert, siltstone, gray quartzite, greenstone, and minor limestone; Ttsl, tuff, sedimentary rocks, and lava (Coats, 1987). WT, west trench; ET, east trench.

ACTIVE FAULTING AND MINERALIZATION

Localizing fluid migration and generation of fault-related gold deposits can be caused by earthquake behavior along active fault zones (Cox, 2005; Sibson et al., 1988). This is in part related to earthquake ruptures and their associated aftershocks that may trigger re-activation of pre-existing shear zones and cause rupture along subsidiary faults within the damage zone (Micklethwaite, 2007). This process has the potential to increase permeability through the depth of the crust creating favorable conditions for fluid-rock interaction, fluid mixing, and migration of mineralization. Coulomb stress transfer modeling of mineralized fossil fault systems indicates that gold deposits are spatially correlated with areas where aftershock clusters along active fault systems have occurred repeatedly (Cox and Ruming, 2004; Micklethwaite and Cox, 2004; 2006). Aftershocks associated with large earthquakes generate rupture on a wide range of related subsidiary faults within the damage zone that have variable sense of slip and orientation. For example, the 1989 Mw7.1 Loma Prieta earthquake in California was associated with aftershocks with strike-slip, thrust, and normal focal mechanisms (Beroza and Zoback, 1993). Aftershocks are generally small-displacement faulting events that occur in close proximity to each other (Kilb and Rubin, 2002). This is significant for gold deposit distribution because the majority of mineralized faults and shears are small-displacement or small-length structures relative to longer unmineralized regional-scale structures (Eisenlohr et al., 1989).

Large magnitude surface-rupturing earthquakes are typically ≥8 km in length and have magnitudes ≥6.0–6.5. These earthquakes rupture through the seismogenic crust into the brittle ductile transition zone influencing fluid flow and permeability over large areas. In Nevada, the Basin and Range topography is generated by active normal faulting along range-front fault systems. Many of these range-front fault systems are associated with scarps in Quaternary deposits indicating relatively youthful displacements. Thus, understanding the distribution of these active fault systems, their interaction with ancient shear zones, as well as their kinematics can lead to insight into the distribution of gold mineralization and deposits.

BEDROCK GEOLOGY, GEOMORPHOLOGY, AND QUATERNARY FAULTS OF THE PROJECT SITE AREA

Bedrock Geology

Bedrock geologic investigations in the project site area have been conducted for over 100 years (i.e., King, 1878); however, the most comprehensive map compilations of the bedrock geology are the product of late twentieth century mapping efforts including Granger et al. (1957), Hope (1970), Hope and Coats (1976), and Stewart and Carlson

(1976). Coats (1987) compiled information from these previous efforts and conducted new mapping resulting in a comprehensive geologic map of Elko County.

In western Elko County, Coats (1987) grouped Paleozoic rocks of the Ordovician, Silurian, and Devonian systems into a single unit (the western assemblage) and indicated that the Vinini and Valmy Formations are the most widespread bedrock units. The Vinini Formation was divided into Early Ordovician quartzite, limestone, calcareous sandstone, siltstone, shale, and minor andesitic tuffs and flows and Middle Ordovician bedded chert and black shale. The Valmy Formation is time equivalent to the Vinini Formation and includes a higher percentage of massive quartzite, chert, and volcanic material (Coats, 1987). Devonian black quartzite, chert, shale, and clastic limestone were defined northeast and north of the project area in the Tuscarora and Mount Blitzen 15 ' quadrangles, respectively.

Within the project area, Coats (1987) mapped two primary bedrock units including (1) Dos; Devonian mudstone, shale, chert, siltstone, gray quartzite, greenstone, and minor limestone, and (2) Ttsl; Tertiary tuff, sedimentary rocks, and lava (figure 2C). Although there are no direct age constraints on the age of the Tertiary deposits described by Coats (1987), biotite extracted from rhyolite pumice in a pyroclastic flow interbedded with gravels has been dated at 33.6 ± 1.6 my (K-Ar age)(McKee et al., 1976, sample 34) and has been interpreted to be part of the same formation (Coats, 1987). More detailed bedrock mapping was compiled by Moore et al. (2002), which showed the project area as DSw, Devonian and Silurian Slaven Chert and Elder Formation including gray-green dolomitic siltstone, dark gray shale and chert, feldspathic siltstone and sandstone, and micaceous mudstone, and green, gray, and black chert with shale and argillite partings (Slaven Chert). To the east and west of the project site, Moore et al. (2002), delineated Tertiary deposits (Tmc, Carlin Formation) including weakly consolidated alluvial, lacustrine, and tuffaceous deposits with interbedded coarse gravels with a tuffaceous silty matrix. Moore et al. (2002) also described tuffaceous siltstone and sandstone with a high proportion of glassy, gray ash with pumiceous shards in the Carlin Formation. Geochronologic analyses ($^{40}Ar/^{39}Ar$) indicate an age for the deposits of 14.4–15.1 Ma (Fleck et al., 1998). In this report, we use the nomenclature of Moore et al. (2002) for the bedrock observed in the trenches and depicted on the trench logs.

Geomorphology

The geomorphology of the project area is characterized by gentle rolling topography with bedrock cored hills and narrow alluvial valleys (figures 2B and 3). Topographic elevations range from 5660 to 6124 feet (1725 to 1866 m). A narrow north-south trending ridge extends across the project area in between West trench and East trench. Bedrock of the Slaven Chert Formation outcrops along the crest and upper side slopes of the ridge. The ridge is dissected by numerous cone-shaped headwater catchments that narrow downslope to v-shaped channels tributary to the main alluvial valleys. These channels are ephemeral and were dry during the field investigation. Landslide scars are generally absent and the primary erosional processes are downslope creep. Groundwater piping along upper slopes of the ridge has resulted in removal of fines, leaving bouldery deposits of bedrock detritus in some areas. Inspection of satellite imagery and aerial photographs indicates that surface scarps and other tectonic geomorphic features indicative of active faulting are not present in the project site area.

Quaternary Faults in the Project Site Vicinity

Active deformation in northeastern Nevada is primarily driven by crustal extension accommodated along normal faults, which has resulted in the modern basin and range topography. Tectonic faults in the project site vicinity that show evidence of movement or surface displacement in the Quaternary include the eastern Tuscarora Mountains, eastern Independence Valley, Tuscarora, and Shoshone Range fault zones, the Southeast Sheep Creek Range, Beowawe, Marys Mountain, and Willow Creek faults, as well as several unnamed fault systems in northwestern Squaw Valley, near Willow Creek Reservoir, and near China Camp (figure 1). The majority of these structures have not been studied in detail and little is known about their slip histories and recurrent behavior. However, understanding the location, slip sense, and relative activity of these structures contributes information towards regional structural and geological models. Brief descriptions of the locations and general characteristics of these structures are provided below.

The eastern Tuscarora Mountains fault zone is an east dipping normal fault that extends along the eastern range front of the Tuscarora Mountains from southwest of Taylor Canyon to the vicinity of U.S. Interstate 80 (Coats, 1987; Dohrenwend and Moring, 1991a; 1991b). The southern part of the fault zone is associated with an ~7 km westward step and extends obliquely across the range. Traces of the fault zone juxtapose Paleozoic bedrock against Quaternary and Quaternary-Tertiary alluvium. Although faceted spurs and wineglass canyons are weakly developed, discontinuous east-facing scarps cut piedmont slope deposits in some areas indicating Quaternary activity.

The 42-km-long eastern Independence Valley fault zone is a northwest dipping normal fault that extends along the western range front of the Independence Mountains juxtaposing bedrock against Quaternary alluvium (Coats, 1987; Dohrenwend and Moring, 1991b; Henry et al., 1998). Traces of the fault zone also extend subparallel to the main zone within the range and across the piedmont in eastern Independence Valley where they displace late Pleistocene and undivided Pleistocene alluvium (Dohrenwend and Moring, 1991b).

A

B

Figure 3. A) View to the east of West trench. B) View to the west of East trench.

The north-northeast striking 22-km-long Tuscarora fault zone extends along the eastern piedmont-slope of the Tuscarora Mountains from near the mouth of Dry Canyon to east of Arthur Canyon in western Independence Valley (Coats, 1987; Dohrenwend and Moring, 1991b; Henry et al., 1998). The zone is characterized by short discontinuous traces that that displace early to middle Pleistocene and possibly younger piedmont-slope deposits across northwest- and southeast-facing scarps that form a complex system of horsts and grabens approximately 3.5-km-wide (Ramelli and dePolo, 1993; Henry et al., 1998). Up to several meters of displacement have been documented across individual fault traces (Henry et al., 1998).

The 118-km-long Shoshone Range fault zone separates bedrock of the Shoshone Range from alluvium in Reese River Valley across a prominent range front southeast of Battle Mountain. To the northeast, the fault bounds the Argenta Rim of the Shoshone Range along a prominent rangefront and projects into Boulder Flat where it is characterized by several subparallel strands. Various workers have defined the traces of the fault zone including Ramelli and House, (2000), Ramelli et al., (2001), Pearthree

(1990), dePolo (1998), Wallace (1979), and Dohrenwend and Moring (1991a). The fault zone is geomorphically well-expressed and is characterized by prominent faceted range front escarpments and distributed mid-valley scarps in Boulder and Reese River valleys. Numerous scarps that displace Holocene alluvium were identified by Ramelli and House (2000) and Ramelli et al. (2001). Paleoseismic studies near the mouth of Lewis Canyon have documented multiple event scarps up to 6-8-m-high and a single coseismic surface rupture across Holocene floodplain deposits that postdates 6867 ± 119 cal yr BP (Wesnousky et al., 2005). At another site, north of Lewis Canyon, Wesnousky et al. (2005) determined that the most recent event occurred close to 3317 ± 364 cal yr BP.

The southeast Sheep Creek Range fault is a 46-km-long southeast dipping normal fault that separates relatively flat-lying Tertiary volcanic rock of the Sheep Creek Range from basin deposits of Boulder Valley (Dohrenwend and Moring, 1991a; Wallace, 1979; House et al., 2001; Ramelli et al., 2001). The northernmost mapped trace of the fault projects towards and is within 10 km of the project site. The fault is primarily expressed by the juxtaposition of bedrock and Quaternary alluvium along a steep bedrock escarpment. Several short (~1 km) scarps that displace Quaternary surficial deposits or erosion surfaces were identified by Dohrenwend and Moring (1991a). Ramelli et al. (2001) inferred displacement of a Holocene alluvial fan at one location.

The Beowawe fault is a northwest-dipping 44-km-long normal fault that extends from the vicinity of Beowawe to Richmond Mountain along the subdued western flank of the Tuscarora Mountains (Wallace, 1979; Dohrenwend and Moring, 1991a). In the vicinity of U.S. Interstate 80, the bedrock/Quaternary alluvium contact that marks the trace of the fault is characterized by subdued range front tectonic geomorphology. West of the piedmont-hillslope break in slope, traces of the fault are characterized by discontinuous west-facing scarps on Quaternary deposits or erosion surfaces interpreted to be early to middle Pleistocene and/or late Pleistocene in age (Dohrenwend and Moring, 1991a). Paleoseismic trenching studies by Wesnousky et al. (2005) indicate the occurrence of the penultimate earthquake in the latest Pleistocene (~18,701 ± 582 cal yr B.P.) and the most recent event in the Holocene (~7450 ± 112 cal yr B.P.). These events were associated with ~2 m and ~0.7 m of vertical offset, respectively (Wesnousky et al., 2005).

The Marys Mountain fault is an east-dipping normal fault that extends for 19 km along the eastern front of the Tuscarora Mountains and juxtaposes bedrock on the west against erosionally dissected Miocene tuffaceous sedimentary rocks on the east (Dohrenwend and Moring, 1991a; 1991b; Wallace, 1979). Tectonic geomorphology along the range front is weakly expressed. A general paucity of Quaternary deposits precludes detailed assessment of the faults relative Quaternary displacement history; however, Henry and Faulds (1999) inferred displacement of Pleistocene alluvium.

Several poorly studied faults have been mapped northwest of the project site area. The Willow Creek fault extends along the southeastern margin of Squaw Valley and marks the southeastern border of the late Cenozoic Midas trough, a regional-scale northeast-striking graben (Dohrenwend and Moring, 1991a; 1991b; Coats, 1987; Stewart and Carlson, 1976). A system of east-northeast trending faults (unnamed faults of northwestern Squaw Valley) extends for ~7 km across northwestern Squaw Valley (Dohrenwend and Moring, 1991b; Coats, 1987). A discontinuous system of faults (unnamed fault zone near Willow Creek Reservoir) extends northeast from the low hills southwest of Willow Creek Reservoir and projects into the northwestern Tuscarora Mountains (Coats, 1987; Henry and Boden, 1998). An unnamed fault near China Camp has been described as possibly displacing Quaternary-Tertiary alluvium (Stewart and Carlson, 1976; Coats, 1987). All of these structures are inferred to be Quaternary active normal faults; however, inferences on Quaternary activity is limited to published map relations and detailed studies have not been conducted.

TRENCHING INVESTIGATION

During October 2017, we performed shallow trench investigations through excavation of two east-west oriented ~1450-foot-long exposures (figure 3). The investigation documented bedrock lithology, bedding orientations (strike and dip), and structural character of faults and discontinuities including orientation, degree of shearing, and presence/absence of secondary mineralization. The degree of Quaternary soil development was also evaluated. The trenches were documented using standard trench logging techniques. A horizontal string grid was installed across each exposure and five foot intervals were marked on the wall. Logs of the exposures were compiled on graph paper with mylar overlays at a scale of 1 inch:5 feet. Final logs were produced using computer graphics software.

West trench was excavated for a distance of 1445 feet (440.4 m) along a west facing slope east of the county road (figure 2). East trench was excavated for a distance of 1490 feet (454.15 m) along the east side of the topographic ridge that bisects the project area and across a small alluvial valley (figure 2). Photographs of trench stratigraphy and structure from selected locations in West trench and East trench are presented in Appendix 1 and 2, respectively. Complete trench logs for West trench and East trench are presented in Plates 1–6 and 7–12, respectively. Specific observations on discontinuities, faults, joints, and bedding are summarized in table 1. The location of bedrock contacts and significant faults are shown on figure 4.

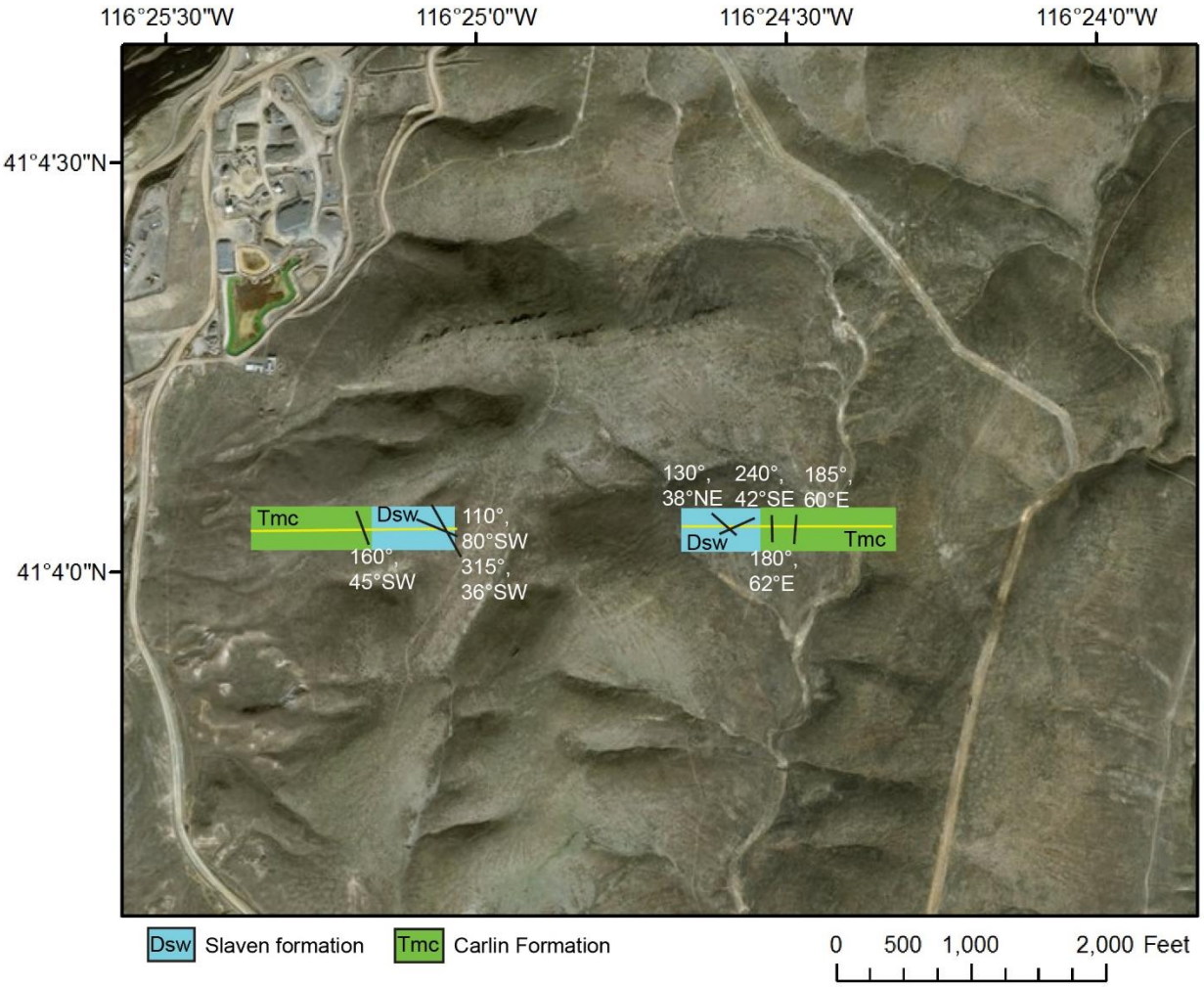

Figure 4. Satellite image of the field site showing bedrock contacts and orientations of significant faults identified in trenches. Trench footprints shown by yellow lines. Other discontinuities, faults, joints, and bedding are listed in Table 1 and delineated on the trench logs (Plates 1–6 and 7–12).

TRENCH RESULTS

West Trench

West trench exposed bedrock of the Carlin and Slaven Chert Formations, as well as a late Pleistocene debris flow. The Carlin Formation extends from the base of the slope (zero feet/m) to 920 feet (280.4 m) where it is in depositional contact with the Slaven Chert Formation. Along this length, the Carlin Formation consists of massive tuffaceous silt, tuffaceous silt with gravel and cobbles, and silty sand with gravel and cobbles. In some zones, the Carlin Formation is crudely bedded and basal contacts of channel deposits are clearly defined. Clasts within the Carlin Formation are predominantly black chert derived from the underlying Slaven Chert Formation. The stratigraphy is interpreted to be lacustrine, lacustrine marginal, fluvial, alluvial, and colluvial in origin. The Slaven Chert Formation extends from 920 feet (280.4 m) to the eastern end of the trench at 1445 feet (440.4 m) and is characterized by thinly bedded black chert and gray siltstone. Bedding of the chert and siltstone is typically on the order of 1–3 inches (2.5–7.6 cm) thick; however, some beds are up to several feet thick. The bedding is folded and intensely sheared. A late Pleistocene debris flow deposit overlies the Slaven Chert Formation between 1175 and 1325 feet (358.1–403.9 m). The debris flow is characterized by alternating layers of matrix supported subangular cobbles and boulders in a silty sand matrix, clast supported layers of 3 inch to 1 foot (7.6–30.5 cm) diameter cobbles, and clast supported pebble gravel. A late Pleistocene soil overlies the entire exposure. The soil consists of gray brown A and Bw horizons of silt loam with gravel and cobbles and a textural B (Bt) horizon characterized by 6-in-long (15.2 cm) prismatic peds, silty clay texture, and dark brown color. The soil is about 1.5 feet (.5 m) thick but thickens between 850 and 435 feet (259–132.5 m) to a maximum thickness of ~4.5 feet (1.4 m). Carbonate stringers within bedrock below the Bt horizon represent 2Ck horizons of the soil profile. Although the age of the soil is unknown, the thickness and texture indicate that it may be older than late Pleistocene.

Table 1. Orientations of bedding, faults, and joints from West trench and East trench. Feature number corresponds to numbered features on trench logs.

Feature	Feature Number	Location	Orientation	Notes
West Trench				
Fault/shear zone	21	895 feet	160°, 45°SW	Hydrothermal alteration, 1 ft (30.5 cm) wide zone of orange colored alteration and 1–2 in (2.5–5 cm) thick $CaCO_3$ along plane. Photo Appendix 1J.
Discontinuity/fault (?)	22	1150 feet	N.A.	Different bedding orientations on each side suggest fault; however, plane is tight with no filling.
Fault (?)	23	1312 feet	110°, 80°SW	Iron oxide along discontinuity. Photo Appendix 1Q.
Fault	24	1430 feet	330°, 38°W	Hydrothermal alteration, 0.5–1 in (1.3–2.5 cm) filling of $CaCO_3$, 0.5 ft (15.2 cm) wide zone of crushed rock. Photo Appendix 1R.
East Trench				
Zone of closely spaced joints or fractures	1	Between 975 and 985 feet	151°, 69°NE 150°, 65°NE 153°, 62°NE	Joints/fractures bound blocks of rock ~1–2 ft (30.5–61 cm) in width. No filling or mineralization. Could be mechanically fractured during excavation.
Joint	2	985 feet	170°, 60°NE 180°, 62°NE	1–2 in (2.5–5 cm) thick $CaCO_3$ seam.
Joint	3	928 feet	N.A.	Ground water barrier across joint, color difference across sharp boundary, tight, no mineralization, no filling.
Joint	4	775 feet	N.A.	Tight joint, no fillings.
Joint	5	792 feet	185°, 60°E	1 in (2.5 cm) thick $CaCO_3$ seam thinning downward to tight rock.
Bedding	6	1052 feet	252°, 40°NW	Thinly bedded chert and siltstone.
Bedding	7	1060 feet	225°, 45°NW	Thinly bedded chert and siltstone.
Bedding	8	1158 feet	266°, 40°NW	Thinly bedded chert and siltstone adjacent to $CaCO_3$ seam.
Bedding	9	1185 feet	130°, 54°NE	Thinnly bedded chert and siltstone. Near Photo Appendix 2K.
Fault	10	1195 feet	N.A.	Conjugate shears. Crushed rock in 1–2 in (2.5–5 cm) zone with manganese, iron, and $CaCO_3$.
Discontinuity	11	1245 feet	N.A.	Zone of parallel $CaCO_3$ seams.
Discontinuity/fault (?)	12	1265 feet	240°, 42°SE 235°, 45°SE	Mineral alteration along plane (manganese, iron). Photo Appendix 2L.
Bedding	13	1287 feet	254°, 54°NW	Thinly bedded chert and siltstone.
Discontinuity	14	1295 feet	229°, Vertical	Thin $CaCO_3$ coating on plane.
Discontinuity/fault (?)	15	1330	N.A.	6 in (15.2 cm) wide zone of crushed rock with alteration.
Bedding	16	1340 feet	249°, 54°NW	Thinly bedded chert and siltstone. Photo near Appendix 2M.
Fault	17	1345 feet	130°, 38°NE	One foot (30.5 cm) wide zone of crushed rock. Photo Appendix 2M.
Discontinuity	18	1385 feet	N.A.	$CaCO_3$ seam along bedding.
Fault	19	1405 feet	N.A.	$CaCO_3$ seam along zone of crushed rock.
Joint	20	1450 feet	230°, 80°NW	Thin $CaCO_3$ on joint plane.

Three faults were identified in the Slaven Chert Formation in West trench including features 22, 23, and 24 (table 1, plates 1 and 2, appendix 1Q and 1R). These faults generally separate differing bedrock orientations and are associated with hydrothermal alteration, crushed rock, carbonate seams, and secondary mineralization including iron oxide and manganese. Bedding plane shears are pervasive within the Slaven Chert Formation and typically associated with carbonate fillings. Many other minor shears and joints were also observed. Another fault was observed within the Carlin Formation (feature 21) and is characterized by hydrothermal alteration and a 1–2 inch (2.5–5 cm) wide carbonate seam along the plane (table 1, plate 3, appendix 1J). None of these faults displace the soil providing evidence that the faulting occurred prior to soil development. This is consistent with the surficial geomorphic observations that indicate the lack of tectonic geomorphic features in the landscape.

East Trench

The bedrock stratigraphy exposed in East trench is similar to West trench. The Carlin Formation is exposed from zero to 255 feet (0–77.7 m) and 294 to 1044 feet (89.6–318.2 m) where it is characterized as tuffaceous silt with gravel and cobbles, massive silt, and matrix supported pebble gravels. The sediments are consistent with colluvial, alluvial, lacustrine, and fluvially reworked lacustrine deposits. A late Pliestocene valley fill deposit overlies the Carlin Formation between 255 and 315 feet (77.7–96 m). The valley fill deposit consists of silty sand with cobbles and subangular boulders up to 1 foot (30.5 cm) diameter. Intensely sheared and folded interbedded chert and siltstone of the Slaven Chert Formation extends from 1044 feet (318.2 m) to the western end of the trench at 1490 feet (454.5 m). A well-developed late Pleistocene soil extends across the entire exposure. The soil is similar to the soil exposed in West trench and consists of loose gray brown silt loam A and Bw horizons and a sandy clay Bt horizon characterized by large blocky prismatic peds and dark brown color. Sub-horizontal carbonate stringers penetrate up to 1 foot (30.5 cm) into the underlying bedrock representing a 2Ck soil horizon. The soil is likely older than late Pleistocene in age.

Bedrock bedding in East trench ranges in strike from 225° to 266° and dips around 40°NW, although folded beds dip to the NE in some places. Five faults were identified in East trench including Features 10, 12, 15, 17, and 19 (table 1, plates 11 and 12, appendix 2L). Each of these faults is associated with crushed rock and secondary mineralization including manganese, iron, and carbonate. Numerous joints and other discontinuities are also evident in the East trench exposure (table 1). Similar to West trench, the observed structures do not displace the soil indicating that faulting occurred prior to soil development.

SUMMARY OF INVESTIGATION

This investigation included the evaluation of regional tectonic geomorphology and documentation of stratigraphic and structural relations exposed in two trenches excavated at the project site located within the Santa Renia Fields 7.5' topographic quadrangle about 45 mi (72 km) north of Carlin, Nevada. The trenching effort focused on identifying and documenting the bedrock stratigraphy and the location and character of faults and other discontinuities.

A wide variety of Quaternary active faults initially formed in the latest Eocene occur in the vicinity of the project site and may influence gold mineralization in the region. These faults are generally north-east trending normal faults and occur to the southeast and northwest of the project area. The southeast Sheep Creek Range fault and the Tuscarora fault zone project towards, but are not mapped through the site. Although evidence for active surface faulting was not observed in the project site area, earthquakes along these faults could influence stress transfer and minor deformation in the project vicinity.

The trenches (West trench and East trench) exposed two primary bedrock units including the Devonian Slaven Chert Formation and the Miocene Carlin Formation. The documentation of the depositional contact between these units provides information to help refine bedrock mapping in the site area. Numerous small displacement faults, joints, and other discontinuities were identified in each trench (primarily in the Slaven Chert Formation) and are typically associated with crushed rock and secondary mineralization. The Slaven Chert Formation rocks are intensely folded and associated with bedding plane faults commonly associated with carbonate seams. Alluvial and fluvial deposits of the Carlin Formation were originally deposited flat, but presently dip slightly indicating uplift and/or folding that postdates the Miocene.

A well-developed Quaternary soil profile characterized by a thick, sandy clay Bt horizon has developed in surficial slope-creep deposits across both exposures and penetrates the bedrock where it is characterized by carbonate stringers sub parallel to the surface. This soil is likely older than late Pleistocene in age and is not displaced by any of the faults within the bedrock, indicating that the faulting predates soil development (>late Pleistocene).

CLOSURE AND LIMITATIONS

The results and conclusions discussed in this report are based on our reconnaissance air photo and satellite imagery evaluation and a limited two week study of the trench exposures. Bedrock mapping was not conducted outside the boundaries of the trench footprints; however, the bedrock contacts mapped in the trench exposures provide a refinement of previous mapping efforts. The length of the

trenches and the allocated field time limited our ability to comprehensively characterize bedding attitudes throughout the trenches. Because the identified faults are sinuous and associated with relatively small displacements, projection of these structures to depth is uncertain.

ACKNOWLEDGMENTS

This project was supported through a research agreement between the Open Pit Mine Exploration (Mine X) group of Barrick Goldstrike Mine and University of Nevada, Reno. Gratitude is extended to Jim Byars, Dexter Race, and Ken Coleman of Barrick Goldstrike Mine for facilitating logistics, field support, and sharing some preliminary mapping of the site vicinity.

REFERENCES

Beroza, G.C., and Zoback, M.D., 1993, Mechanism diversity of the Loma Prieta aftershocks and mechanisms for mainshock-aftershock interaction: Science, v. 259, p. 210–213.

Coats, R.R, 1987, Geology of Elko County, Nevada: Nevada Bureau of Mines and Geology Bulletin 101, 112 p., 1 plate, scale 1:250,000.

Cox, S.F., 2005, Coupling between deformation, fluid pressures, and fluid flow in ore-producing hydrothermal systems at depth in the crust: Economic Geology 100th Anniversary Volume, p. 1–35.

Cox, S.F., and Ruming, 2004, The St. Ives mesothermal gold system, western Australia—a case of golden aftershocks?: Journal of Structural Geology, v. 26, p. 1109–1125.

dePolo, C.M., 1998, A reconnaissance technique for estimating the slip rate of normal-slip faults in the Great Basin, and application to faults in Nevada, U.S.A.: Reno, University of Nevada, unpublished Ph.D. dissertation, 199 p.

Dohrenwend, J.C., and Moring, B.C., 1991a, Reconnaissance photogeologic map of young faults in the Winnemucca 1° by 2° quadrangle, Nevada: U.S. Geological Survey Miscellaneous Field Studies Map MF-2175, 1 sheet, scale 1:250,000.

Dohrenwend, J.C., and Moring, B.C., 1991b, Reconnaissance photogeologic map of young faults in the McDermitt 1° by 2° quadrangle, Nevada, Oregon, and Idaho: U.S. Geological Survey Miscellaneous Field Studies Map MF-2177, 1 sheet, scale 1:250,000.

Eisenlohr, B.N., Groves, D., and Partington, G.A., 1989, Crustal-scale shear zones and their significance to Archean gold mineralization in western Australia: Mineralium Deposita, v. 24, p. 1–8.

Fleck, R.J., Theodore, T.J., Sarna-Wojcicki, A., and Meyer, C.E., 1998, Age and possible source of air-fall tuffs of the Miocene Carlin Formation, northern Carlin trend, *in* Tosdal, R.M., editor, Contributions to the gold metallogeny of northern Nevada: U.S. Geological Survey Open-File Report 98-338, p. 176–192.

Granger, A.E., Bell, M.M., Simmons, G.C., and Lee, F., 1957, Geology and mineral resources of Elko County, Nevada: Nevada Bureau of Mines and Geology Bulletin 54, 190 p.

Henry, C.D., Boden, D.R., and Castor, S.B., 1998, Geologic map of the Tuscarora quadrangle, northern Nevada: Nevada Bureau of Mines and Geology Open-File Report 98-AA, scale 1:24,000.

Henry, C.D., and Boden, D.R., 1998, Geologic map of the Toe Jam Mountain quadrangle, Nevada: Nevada Bureau of Mines and Geology Open-File Map 98-BB, scale 1:24,000.

Henry, C.D., and Faulds, J.E., 1999, Geologic map of the Emigrant Pass quadrangle, Eureka County, Nevada: Nevada Bureau of Mines and Geology Open-File Report 99-9, scale 1:24,000.

Hope, R.A., 1970, Preliminary geologic map of Elko County, Nevada: U.S. Geological Survey Open-File Map, scale 1:200,000.

Hope, R.A., and Coats, R.R, 1976, Preliminary geologic map of Elko County, Nevada: U.S. Geological Survey Open-File Report 76-779, scale 1:100,000.

House, P.K., Ramelli, A.R., and Wrucke, C.T., 2001, Geologic map of the Argenta quadrangle, Lander County, Nevada: Nevada Bureau of Mines and Geology Open-File Report, scale 1:24,000.

Kilb, D., and Rubin, A.M., 2002, Implications of diverse fault orientations imaged in relocated aftershocks of the Mount Lewis, ML 5.7, California earthquake: Journal of Geophysical Research, v. 107, B11, doi:10.1029/2001JB000149, 17 p.

King, C., 1878, Systematic geology—geological exploration of the fourtieth parallel, v. 1: Washington D.C. U.S. Government Printing Office, 803 p.

McKee, E.H., Tarshis, A.L., and Marvin, R.F., 1976, Summary of radiometric ages of Tertiary volcanic and selected plutonic rocks in Nevada, part V—northeastern Nevada: Isochron/West, no. 16, p. 15–27.

Micklethwaite, S., 2007, The significance of linear trends and clusters of fault-related mesothermal lode gold mineralization: Economic Geology, Scientific Communications, v. 102, p. 1157–1164.

Micklethwaite, S., and Cox, S.F., 2004, Fault-segment rupture, aftershock-zone fluid flow, and mineralization, Geology: v. 32, p. 813–816.

Micklethwaite, S., and Cox, S.F., 2006, Progressive fault triggering and fluid flow in aftershock domains—examples from mineralized Archaean fault systems, Earth and Planetary Science Letters, v. 250, p. 318–330.

Moore, S. (geologic editor), Goings M., Renas, J.J., and Tingley, S. (cartographic compilers), 2002, Geology of the northern Carlin trend, Plate 1, *in* Thompson, T.B., Teal, L., and Meeuwig, R.O., editors, 2002, Gold deposits of the Carlin trend: Nevada Bureau of Mines and Geology Bulletin 111, 204 p., 3 plates.

Pearthree, P.A., 1990, Geomorphic analysis of young faulting and fault behavior in central Nevada: Tucson, University of Arizona, unpublished Ph.D. dissertation, 212 p.

Ramelli, A.R., and dePolo, C.M., 1993, Examples of Holocene and latest Pleistocene faulting in northern and eastern Nevada: Geological Society of America Abstracts with Programs, v. 25, no. 5, p. 136.

Ramelli, A.R., and House, P.K., 2000, Geologic map of the Bateman Spring quadrangle, Lander County, Nevada: Nevada Bureau of Mines and Geology Open-File Report 00-8, scale 1:24,000.

Ramelli, A.R., House, P.K., Wrucke, C.T., and John, D.A., 2001, Geologic map of the Stony Point quadrangle, Lander County, Nevada: Nevada Bureau of Mines and Geology Map 131, scale 1:24,000.

Ressel, M.W. and Henry, C.D., 2006, Igneous geology of the Carlin trend, Nevada—development of the Eocene plutonic complex and significance for Carlin-type gold deposits: Economic Geology, v. 101, p. 347–383.

Sibson, R.H., Robert, F., and Poulsen, K.H., 1988, High-angle reverse faults, fluid pressure cycling, and mesothermal gold deposits: Geology, v. 16, p. 551–555.

Stewart, J.H., and Carlson, J.E., 1976, Geologic map of north-central Nevada: Nevada Bureau of Mines and Geology Map 50, scale 1:250,000.

Teal, L., and Jackson, M., 2002, Geologic overview of the Carlin trend gold deposits, *in* Thompson, T.B., Teal, L., and Meeuwig, R.O. editors, 2002, Gold deposits of the Carlin trend: Nevada Bureau of Mines and Geology Bulletin 111, 204 p., 3 plates.

Teal, L., and Jackson, M., 1997, Geologic overview of the Carlin trend gold deposits and description of recent deep discoveries, *in* Vikre, P., Thompson, T.B., Bettles, K., Christensen, O., and Parratt, R., editors, Carlin-type gold deposits field conference: Society of Economic Geologists Guidebook Series, v. 28, p. 3–37.

Wallace, R.E., 1979, Map of young fault scarps related to earthquakes in north-central Nevada: U.S. Geological Survey Open-File Report 79-1554, 2 sheet, scale 1:125,000.

Wesnousky, S.G., Barron, A.D., Briggs, R.W., Caskey, S.J., Kumar, Senthil, and Owen, L., 2005, Paleoseismic transect across the northern Great Basin: Journal of Geophysical Research, v. 110, B05408, 25 p.

Suggested Citation:

Koehler, R.D., and Chupik, C.M., 2018, Subsurface trenching investigation in support of the Barrick Goldstrike N. Carlin Trend Structure Project: Nevada Bureau of Mines and Geology Open-File Report 18-2, 12 plates, scale 1:60, 18 p.

© Copyright 2018 The University of Nevada, Reno. All Rights Reserved.

APPENDIX 1

West Trench

Photographs from selected locations.

Appendix 1A. Photograph from location 40 feet in West trench showing tuffaceous silt interpreted to be lacustrine in origin overlain by gravel and cobble with a tuffaceous silt matrix interpreted to be lacustrine marginal colluvium of the Carlin Formation.

Appendix 1B. Photograph from location 70 feet in West trench showing gravel and cobble silt with a tuffaceous silt matrix interpreted to be lacustrine marginal colluvium of the Carlin Formation.

Appendix 1C. Photograph from location 150 feet in West trench showing tuffaceous silt of the Carlin Formation. Deposits are interpreted to be lacustrine in origin based on thin laminae and sandy layers (<0.5 inch width). A sharp discontinuity separates similar deposits (gray on the east and tan orange on the west) possibly related to groundwater differences.

Appendix 1D. Photograph from location 290 feet in West trench showing gravel to cobble silt with tuffaceous silt matrix interpreted to be lacustrine marginal colluvium of the Carlin Formation.

Appendix 1E. Photograph from location 360 feet in West trench showing tuffaceous lacustrine silt overlain by gravel to cobble tuffaceous silt colluvium of the Carlin Formation. Thin carbonate stingers within the colluvium are related to soil formation.

Appendix 1F. Photograph from location 440 feet in West trench showing basal colluvium consisting of ~40% angular chert clasts averaging 1–3 inches in diameter overlain by gravelly silt colluvium of the Carlin Formation.

Appendix 1G. Photograph from location 630 feet in West trench showing gravelly silt lacustrine deposits of the Carlin Formation overlain by soil characterized by a thick textural B horizon with prismatic structure.

Appendix 1H. Photograph from location 755 feet in West trench showing gravelly silt lacustrine or colluvial deposits of the Carlin Formation overlain by a thick textural B soil horizon characterized by well-developed ped structure (prismatic, 10 cm size).

Appendix 1I. Photograph from location 855 feet in West trench showing angular gravel to cobble silt (clasts up to 6 inches in length) overlain by tuffaceous silt with prominent carbonate stringers related to soil development.

Appendix 1J. Photograph from location 895 feet in West trench showing tuffaceous gravelly silt with angular clasts of chert up to 6 inches but averaging 1–2 inches. Sharp discontinuity characterized by 1–2 inches of carbonate along plane and a 1–1.5 feet thick zone of hydrothermal alteration above plane. Matrix is orange brown and pinkish brown west and east of discontinuity, respectively.

Appendix 1K. Photograph from location 920 feet in West trench showing depositional contact between thinly bedded chert and siltstone of the Slaven Chert Formation and tuffaceous silt (~20% angular chert clasts) of the Carlin Formation.

Appendix 1N. Photograph from location 1200 feet in West trench showing thinly bedded (2–4 inches) gray siltstone altered to orange and red colors.

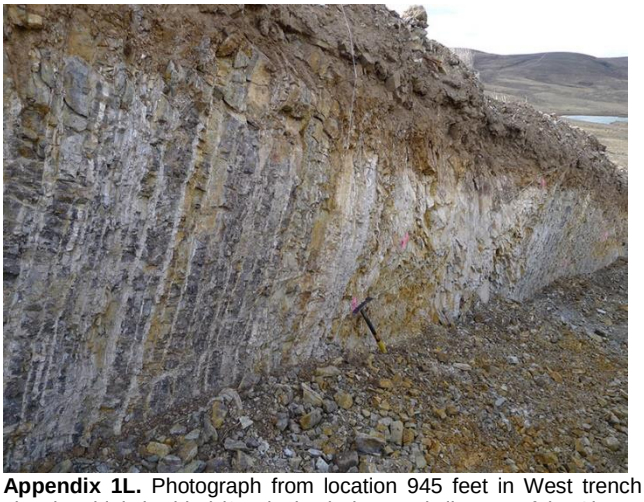

Appendix 1L. Photograph from location 945 feet in West trench showing thinly bedded (3–4 inches) chert and siltstone of the Slaven Chert Formation. Beds become 6 to 8 inches thick towards the western side of photo.

Appendix 1O. Photograph from location 1220 feet in West trench showing interbedded black chert and orange siltstone of the Slaven Chert Formation overlain by a Quaternary clast supported pebble to cobble debris flow deposit.

Appendix 1M. Photograph from location 1030 feet in West trench showing thinly bedded (3–4 inches) black chert and gray brown siltstone of the Slaven Chert Formation.

Appendix 1P. Photograph from location 1300 feet in West trench showing gray siltstone of the Slaven Chert Formation overlain by erosional unconformity and Quaternary pebble to cobble debris flow deposit.

Appendix 1Q. Photograph from location 1310 feet in West trench showing interbedded black chert and orange and gray siltstone of the Slaven Chert Formation. Carbonate lined discontinuity separating slightly different bedrock orientations indicates presence of fault.

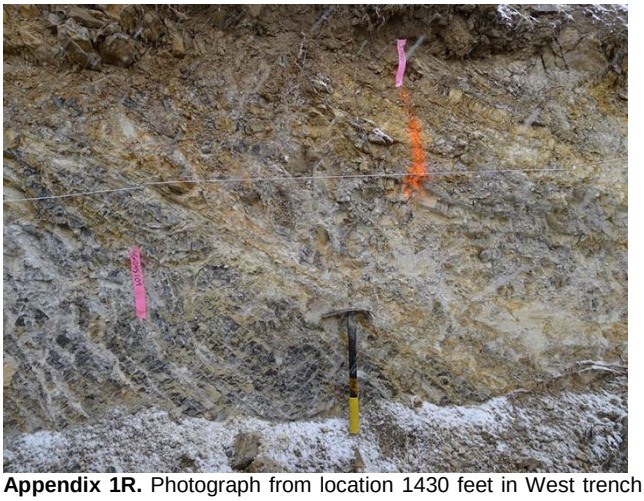

Appendix 1R. Photograph from location 1430 feet in West trench showing discontinuity separating thinly bedded black chert on the east from predominantly siltstone on the west. Discontinuity associated with hydrothermal alteration and 0.5–1 inch of carbonate along the plane.

APPENDIX 2

East Trench

Photographs from selected locations.

Appendix 2A. Photograph from location zero feet in East trench showing sand and silt with gravel and cobbles of the Carlin Formation. Cobbles are up to 1 foot in long dimension but generally average about 6 inches long. Cobbles are subangular and predominantly chert. Well-developed Bt soil horizon overlies the Carlin Formation.

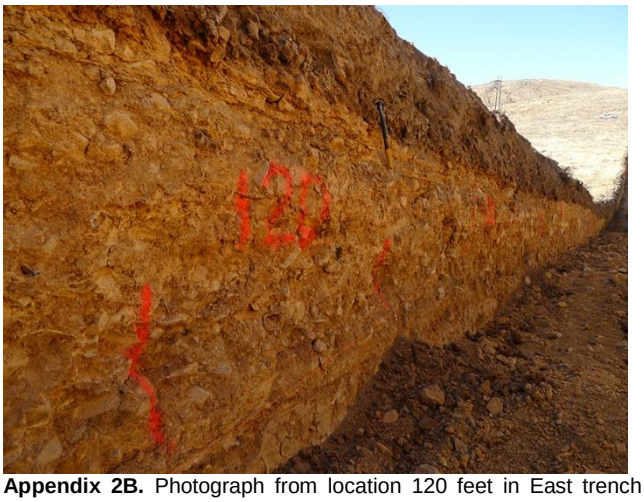

Appendix 2B. Photograph from location 120 feet in East trench showing sand and silt with gravel and cobbles of the Carlin Formation. Crude bedding suggest an alluvial origin. Carbonate stringers parallel the base of the soil indicating deep soil development.

Appendix 2C. Photograph from location 250 feet in East trench showing contact between alluvial deposits of the Carlin Formation (left) and late Pleistocene valley fill deposits (right). The valley fill deposits consist of sand with cobbles and subangular boulders up to 1 foot long dimension.

Appendix 2D. Photograph from location 420 feet in East trench showing lacustrine to fluvial facies of the Carlin Formation including tuffaceous silt and thin alluvial gravel to cobble layers. Clasts are predominantly chert in alluvial layers.

Appendix 2E. Photograph from location 630 feet in East trench showing tuffaceous alluvium of the Carlin Formation. Large cobbles indicate a high energy alluvial origin.

Appendix 2F. Photograph from location 750 feet in East trench showing massive tuffaceous silt of the Carlin Formation possibly lacustrine in origin. Subtle channels with gravel and cobbles occur immediately east of 750 feet indicating a possible lacustrine marginal stream system.

Appendix 2G. Photograph from location 880 feet in East trench showing lacustrine tuffaceous silt at the base of the exposure overlain by alluvial sand with gravels and cobbles of the Carlin Formation. Well-developed soil Bt horizon with large columnar to prismatic peds overlies the Carlin Formation.

Appendix 2H. Photograph from location 930 feet in East trench showing discontinuity (joint) which creates a groundwater barrier. Tuffaceous silt of the Carlin Formation is light tan on the left and brown on the right. Discontinuity is tight with no filling or mineralization.

Appendix 2I. Photograph from location 1040 feet in East trench showing depositional contact between tuffaceous silt of the Carlin Formation and thinly bedded chert and siltstone of the Slaven Chert Formation. The contact is characterized by a zone of carbonate 1–2 inches thick.

Appendix 2J. Photograph from location 1140 feet in East trench showing thinly bedded chert of the Slaven Chert Formation and synclinal folding.

Appendix 2K. Photograph from location 1190 feet in East trench showing fault in Slaven Chert Formation chert. Fault is characterized by 1 inch wide zone of crushed rock that widens upward to ~1 foot width.

Appendix 2L. Photograph from location 1260 feet in East trench showing mineralized fault plane in the Slaven Chert Formation. Mineralization includes manganese, iron, and carbonate.

Appendix 2M. Photograph from location 1345 feet in East trench showing fault in Slaven Chert Formation. Fault characterized by 1 foot wide zone of crushed rock.

Appendix 2N. Photograph from location 1370 feet in East trench showing shear fabric that cross cuts bedding in the Slaven Chert Formation.

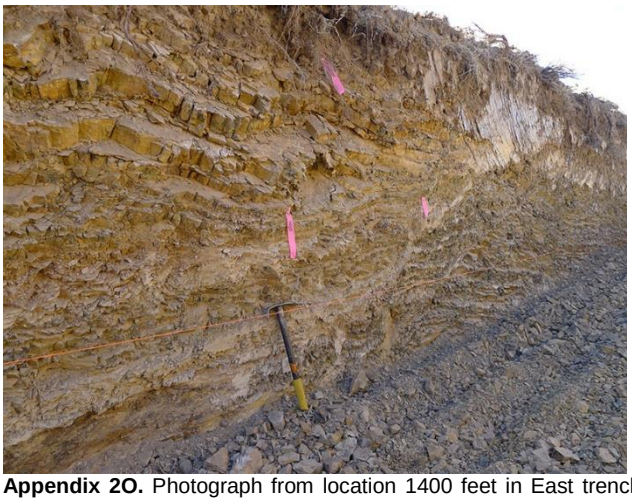

Appendix 2O. Photograph from location 1400 feet in East trench showing fault in the Slaven Chert Formation characterized by shear fabric that cuts across bedding.